Physica A 421 (2015) 54–68

Contents lists available at ScienceDirect

Physica A

journal homepage: www.elsevier.com/locate/physa

A dynamical analysis of allele frequencies in populations evolving under assortative mating and mutations

David M. Schneider [a,*], Eduardo do Carmo [b], Marcus A.M. de Aguiar [a]

[a] Instituto de Física 'Gleb Wataghin', Universidade Estadual de Campinas, Unicamp, 13083-859, Campinas, SP, Brazil
[b] Universidade Federal da Integração Latino Americana, 85867-970, Foz do Iguaçu, PR, Brazil

HIGHLIGHTS

- A resolution of the dynamics of a population of two biallelic loci individuals evolving under assortative mating and mutations is provided.
- A bifurcation diagram is constructed to describe the dynamics in a qualitative way.
- The fate of initial conditions is obtained by the employment of a constant of motion.
- A trade-off between assortativity and the effect of mutations is discussed.

ARTICLE INFO

Article history:
Received 11 June 2014
Received in revised form 29 October 2014
Available online 15 November 2014

Keywords:
Population genetics
Modes of speciation
Assortativity
Bifurcation analysis

ABSTRACT

We study the evolution of allele frequencies for infinitely large populations subjected to mutations and assortative mating. Haploid individuals are described by two biallelic genes, and assortativity is introduced by preventing mating between individuals whose alleles differ at both loci. In the absence of mutations, evolution leads to the disappearance of one of the alleles. However, a particular combination of the allele frequencies at the two loci is maintained constant. We show that this combination remains constant even when mutations are present, revealing the robustness of the epistatic correlation introduced by the non-random mating mechanism. We obtain the equilibrium solutions for arbitrary values of the mutation rate and provide a description of the dynamics on the basis of a bifurcation analysis.

1. Introduction

The concept of species is deeply rooted in the idea of reproductive isolation: groups of individuals form separate species if individuals belonging to different groups are unable to generate fertile offspring through mating [1–3]. Such isolation prevents genetic modifications occurring in one group to spread to other groups, causing their evolution to follow relatively independent paths. Understanding the genetic and ecological mechanisms that lead to the emergence of reproductive isolation is, therefore, a fundamental quest of evolutionary theory.

In a series of recent papers [4–6] it has been shown that speciation may occur spontaneously in spatially extended populations where individuals are allowed to mate only if they are close enough and not too different genetically. Mating restriction by genetic similarity, also termed assortative mating, can be modeled by attributing haploid genomes with B

* Corresponding author. Tel.: +55 19 3521 5463.
E-mail address: schneide@ifi.unicamp.br (D.M. Schneider).

http://dx.doi.org/10.1016/j.physa.2014.11.030
0378-4371/

biallelic loci to individuals and allowing them to mate only if the genomes differ in no more than G loci [7–9,4,5]. This rule is supported by the idea that individuals have limited tolerance to differences when choosing a mate, so that if the other individual is too different, it will not be considered as a mating option [10].

The model proposed in Ref. [4] considers finite populations, includes mutations and is not panmictic, since mating occurs only between spatially close and genetically similar individuals. Speciation occurs because of the combined effects of isolation by spatial distance [11] and isolation by genetic distance. Individuals are initially identical and differentiation occurs only by mutation and drift. However, as the population diversity increases the genetic constraint aids differentiation by disruptive selection. If G, the maximum allowed genetic distance, is much smaller than B, the total number of genes, mutations may lead to incompatible haplotypes. Analytical expressions indicating when speciation is possible under these conditions were recently obtained [12,13], but the contribution of the genetic mating restriction to the process was included as an ansatz based on numerical simulations. The dynamical equations describing the evolution of haplotype frequencies in the general case of B loci and arbitrary G were recently derived and their solutions were obtained in the absence of mutations [14].

In a previous paper [15] we have analyzed in detail the dynamics of allele frequencies for infinitely large populations of haploid individuals not subjected to mutations. We considered the simplest case of two loci, $B = 2$, and $G = 1$, so that individuals whose alleles differ at both loci are considered incompatible and mating does not happen. In this case there are only four haplotypes, AB, Ab, aB and ab, $AB-ab$ and $Ab-aB$ being the incompatible pairs. We derived the evolution equations for the haplotype frequencies $p_{u'u''}$ (with $u' = A$, a and $u'' = B$, b), and found that the coupling between the loci introduced by the restricted mating leads to a strong correlation between the allele frequencies. For $\tilde{p}_A = p_{AB} + p_{Ab}$ the frequency of the allele A and $\tilde{p}_B = p_{aB} + p_{AB}$ the frequency of the allele B, the quantity $T = (\tilde{p}_A - 1/2)/(\tilde{p}_B - 1/2)$ remains constant during the evolution, although $\tilde{p}_A$ and $\tilde{p}_B$ do change. Using this conserved quantity we were able to solve the dynamical equations and show that one of the alleles always disappears from the population.

Models with one or two loci and two alleles have been extensively studied in the past, but focused mostly on selection and not on assortativity [16–21]. A comprehensive review of recent models of assortative mating can be found in Ref. [22]. One-locus diploid models where individuals have equal mating success usually lead to a decrease in the proportion of heterozygotes, going to zero for complete assortativity, where each type mates only with itself [23–25]. One locus models where mating success is frequency dependent have also been considered [26–28] but have also been shown to lead to the extinction of heterozygotes if assortativity is complete. The model considered here is similar to the two-allele two-locus version of the Moore model [22]. In that case, however, the heterozygotes Ab and aB correspond to the same phenotype, which lead to particularly simple and symmetric equilibria. Finally we mention the Higgs–Derrida model [29,30] where loci are unlinked (Ab and aB map to different phenotypes) but which considers the limit of infinitely many loci.

In this paper we extend the results obtained in Ref. [15] to include the effects of mutations. We show that, surprisingly, the function T remains constant for arbitrary values of the mutation rate. We obtain all the equilibrium solutions analytically and find that, contrary to the equilibrium solutions in the absence of mutations, they do not imply the lost of an allele. Instead, they are characterized by the fact that one of the four alleles ends up with a very small frequency, which is given as a function of μ and T (Fig. 3). As μ goes to zero, this allele vanishes and the result of Ref. [15] is recovered. In addition, we find that equilibrium solutions merge at a critical mutation rate. This value of the mutation rate is associated to a stability change and to a biologically meaningful bifurcation. Another bifurcation takes place for negative mutation rates. Not being relevant from a biological point of view, this second bifurcation is illustrative to describe, in addition to the former, the global structure of the phase space.

The paper is organized as follows: in Section 2 we describe the reproductive mechanism in the presence of mutations and derive the haplotype frequencies evolution equations for very general mating schemes. In Section 3 we briefly discuss the random mating scenario. The dynamical implications of the combination of assortativeness and mutations are studied in Section 4. Section 5 presents a qualitative description of the dynamics based on a bifurcation analysis, and Section 6 is devoted to discuss the results and to expose the main conclusions. Complementary technical calculations are added in separated appendices.

2. Reproductive mechanism

Consider a population of hermaphrodite individuals with two biallelic loci. Let A and a denote the alleles at one locus, and B and b the alleles at the other, so that the haplotypes are AB, Ab, aB, and ab. The number of individuals of each type in the generation t is given by N^t_{AB}, N^t_{Ab}, N^t_{aB} and N^t_{ab}, with $N^t_{AB} + N^t_{Ab} + N^t_{aB} + N^t_{ab} = N^t$, the total size of the population. Encounters between the members of this generation may succeed or not in producing offspring for the generation $t + 1$, depending on the probabilities $w_{h_1:h_2}$ (h_1 and h_2 being the parental haplotypes). The rates $w_{h_1:h_2}$ (see Table 1) incorporate both the effects of the compatibility between the parents (sexual selection) and the viability of the newly formed zygote (viability selection). In our model the viability selection is the same for all individuals, and takes place once the zygote was formed through the inheritance of a recombinated chromosome (at a recombination rate r). Assortativeness, represented by the sexual selection component, is described by the compatibility between the parents and acts at a prezygotic level. The reason for adding a postzygotic factor to the compound fitness $w_{h_1:h_2}$, from now on the compatibility–viability selection rate, has the only purpose of keeping the total number of individuals constant across generations, and represents an implicit

Table 1
Encounters between individuals in the generation t that contribute to individuals with haplotype AB in the generation $t+1$.

Parental haplotypes	Number of encounters	Fraction of successful AB offspring encounters
$AB \times AB$	$1/2 \times N_{AB}^t \times (N_{AB}^t - 1)$	$w_{AB:AB} \times (1-\mu)^2$
$AB \times Ab$	$N_{AB}^t \times N_{Ab}^t$	$1/2 \times w_{AB:Ab} \times (1-\mu)$
$AB \times aB$	$N_{AB}^t \times N_{aB}^t$	$1/2 \times w_{AB:aB} \times (1-\mu)$
$AB \times ab$	$N_{AB}^t \times N_{ab}^t$	$[(1-r)/2 - \mu(1-\mu)(1-2r)] \times w_{AB:ab}$
$Ab \times aB$	$N_{Ab}^t \times N_{aB}^t$	$[r/2 + \mu(1-\mu)(1-2r)] \times w_{Ab:aB}$
$Ab \times Ab$	$1/2 \times N_{Ab}^t \times (N_{Ab}^t - 1)$	$w_{Ab:Ab} \times \mu(1-\mu)$
$aB \times aB$	$1/2 \times N_{aB}^t \times (N_{aB}^t - 1)$	$w_{aB:aB} \times \mu(1-\mu)$
$Ab \times ab$	$N_{Ab}^t \times N_{ab}^t$	$1/2 \times w_{Ab:ab} \times \mu$
$aB \times ab$	$N_{aB}^t \times N_{ab}^t$	$1/2 \times w_{aB:ab} \times \mu$
$ab \times ab$	$1/2 \times N_{ab}^t \times (N_{ab}^t - 1)$	$w_{ab:ab} \times \mu^2$

carrying capacity, i.e. finite abundance of resources. Once the new individual is formed, its genome can mutate at a mutation rate μ per gene.

According to Table 1 (see Appendix A for an explanation of the coefficients in the third column), and assuming non-overlapping generations, the number of AB individuals in the generation $t+1$ obeys

$$\begin{aligned} N_{AB}^{t+1} = {} & \frac{N_{AB}^t(N_{AB}^t-1)}{2} w_{AB:AB}(1-\mu)^2 + \frac{N_{AB}^t N_{Ab}^t}{2} w_{AB:Ab}(1-\mu) + \frac{N_{AB}^t N_{aB}^t}{2} w_{AB:aB}(1-\mu) \\ & + N_{AB}^t N_{ab}^t [(1-r)/2 - \mu(1-\mu)(1-2r)] w_{AB:ab} \\ & + N_{Ab}^t N_{aB}^t [r/2 + \mu(1-\mu)(1-2r)] w_{Ab:aB} + \frac{N_{Ab}^t(N_{Ab}^t-1)}{2} w_{Ab:Ab}\mu(1-\mu) \\ & + \frac{N_{aB}^t(N_{aB}^t-1)}{2} w_{aB:aB}\mu(1-\mu) + \frac{N_{Ab}^t N_{ab}^t}{2} w_{Ab:ab}\mu + \frac{N_{aB}^t N_{ab}^t}{2} w_{aB:ab} + \mu + \frac{1}{2} N_{ab}^t(N_{ab}^t-1) w_{ab:ab}\mu^2. \end{aligned} \tag{1}$$

The equations for the remaining haplotypes can be obtained by constructing equivalent tables, or by simply replacing the alleles in Eq. (1) as follows: $B \leftrightarrow b$ to obtain N_{Ab}^{t+1}, $A \leftrightarrow a$ to obtain N_{aB}^{t+1}, and both $B \leftrightarrow b$ and $A \leftrightarrow a$ to obtain N_{ab}^{t+1}.

3. Random mating

Setting $w_{h_i:h_j} = w_{RM}$ for all rates we can calculate the value of w_{RM} by imposing $N_{AB}^t + N_{Ab}^t + N_{aB}^t + N_{ab}^t = N^t \equiv N$ for all times. The right side gives $w_{RM} N^t(N^t-1)/2$, which implies $w_{RM} = 2/(N-1)$.

Equations for the haplotype frequencies

$$p_{AB}^t = N_{AB}^t/N^t \tag{2}$$

$$p_{Ab}^t = N_{Ab}^t/N^t \tag{3}$$

$$p_{aB}^t = N_{aB}^t/N^t \tag{4}$$

$$p_{ab}^t = N_{ab}^t/N^t \tag{5}$$

are obtained by replacing the compatibility–viability selection rate w_{RM} in Eq. (1) (and in the corresponding equations for the other haplotypes) and dividing both sides by N. From now on we will restrict ourselves to the case $r = 1/2$. In the limit of infinitely large populations ($w_{RM} = 2/N$), we obtain

$$p_{AB}^{t+1} = p_{AB}^t(1-\mu) + p_{ab}^t\mu + \Gamma^t\mu(1-\mu) - \frac{1}{2}D^t \tag{6}$$

$$p_{Ab}^{t+1} = p_{Ab}^t(1-\mu) + p_{aB}^t\mu - \Gamma^t\mu(1-\mu) + \frac{1}{2}D^t \tag{7}$$

$$p_{aB}^{t+1} = p_{aB}^t(1-\mu) + p_{Ab}^t\mu - \Gamma^t\mu(1-\mu) + \frac{1}{2}D^t \tag{8}$$

$$p_{ab}^{t+1} = p_{ab}^t(1-\mu) + p_{AB}^t\mu + \Gamma^t\mu(1-\mu) - \frac{1}{2}D^t \tag{9}$$

where

$$D^t \equiv p^t_{AB}p^t_{ab} - p^t_{Ab}p^t_{aB} \tag{10}$$

stands for the genetic linkage disequilibrium. The quantity Γ^t is defined as

$$\Gamma^t \equiv (p^t_{Ab})^2 + (p^t_{aB})^2 - (p^t_{AB})^2 - (p^t_{ab})^2. \tag{11}$$

3.1. Haplotype equilibria and the evolution of allele frequencies

For the case $\mu \neq 0$, the only stable solution is given by the equiprobable distribution $p^t_{AB} = p^t_{Ab} = p^t_{aB} = p^t_{ab} = 1/4$. To demonstrate this assertion we will proceed in two steps. First, we will prove that the equiprobable distribution is the only equilibrium solution of Eq. (6) and, second, that this equilibrium is stable.

The equilibrium conditions applied to Eqs. (6)–(9) lead to

$$0 = -\mu(p^t_{AB} - p^t_{ab}) + \Gamma^t\mu(1-\mu) - \frac{1}{2}D^t \tag{12}$$

$$0 = -\mu(p^t_{Ab} - p^t_{aB}) - \Gamma^t\mu(1-\mu) + \frac{1}{2}D^t \tag{13}$$

$$0 = \mu(p^t_{Ab} - p^t_{aB}) - \Gamma^t\mu(1-\mu) + \frac{1}{2}D^t \tag{14}$$

$$0 = \mu(p^t_{AB} - p^t_{ab}) + \Gamma^t\mu(1-\mu) - \frac{1}{2}D^t. \tag{15}$$

Subtracting Eq. (12) from (15) and (13) from (14) results in

$$p^t_{AB} = p^t_{ab} \quad \text{and} \quad p^t_{Ab} = p^t_{aB}, \tag{16}$$

respectively, which for $\mu \neq 0$ implies $\Gamma^t = -2D^t$. On the other hand, adding Eqs. (12) and (15) (or equivalently (13) and (14)) we obtain

$$0 = 2\Gamma^t\mu(1-\mu) - D^t = -D^t\left[1 + 4\mu(1-\mu)\right], \tag{17}$$

which must hold for any value of the mutation rate μ. As a consequence, in the equilibrium both quantities Γ^t and D^t must vanish and therefore $p^t_{AB} = p^t_{ab} = p^t_{Ab} = p^t_{aB} = 1/4$. Notice that for $\mu = 0$ the only factor that vanishes is the linkage disequilibrium D^t, as pointed out in Ref. [15].

For the stability analysis we take three of the four variables (for instance p^t_{AB}, p^t_{Ab} and p^t_{aB}) together with the normalization constraint, and linearize Eqs. (6)–(9) in the neighborhood of the equiprobable distribution. The stability matrix results in two degenerated eigenvalues $\zeta_{\rm d} = 1 - 2\mu$ and one non-degenerated eigenvalue $\zeta_{\rm nd} = \frac{1}{2}(1-2\mu)^2$. For $0 < \mu < 1$ the eigenvalues satisfy $|\zeta_d| < 1$ and $|\zeta_{\rm nd}| < 1$ so the fixed point is stable.

It is interesting to relate the equilibrium properties of the haplotype frequencies to the allele proportions at the two loci. From the definition of the allele frequencies we recognize that haplotypes are in linkage equilibrium. Namely, as $\tilde{p}_u = 1/4 + 1/4 = 1/2$ (for any allele $u = A, a, B, b$), it follows that $p_{u'u''} = \tilde{p}_{u'}\tilde{p}_{u''}$ (for $u' = A, a$ and $u'' = B, b$). We can also study the time evolution of the allele frequencies by deriving their dynamical equations directly from Eqs. (6)–(9). This yields

$$\tilde{p}^{t+1}_u = \tilde{p}^t_u(1-\mu) + (1-\tilde{p}^t_u)\mu = \alpha\tilde{p}^t_u + \beta \tag{18}$$

with $\alpha = 1 - 2\mu$ and $\beta = \mu$. Successive iterations of (18) give

$$\tilde{p}^t_u = \alpha^t\tilde{p}^0_u + \beta\sum_{k=0}^{t-1}\alpha^k = \alpha^t\tilde{p}^0_u + \beta\frac{1-\alpha^t}{1-\alpha} = (1-2\mu)^t(\tilde{p}^0_u - 1/2) + 1/2. \tag{19}$$

For $\mu = 0$ we obtain the result corresponding to constant proportions for the four alleles. Nevertheless, even for a very small mutation rate allele frequencies exponentially approach the value 1/2 and the population ends up in a completely mixed composition at both loci. The bigger the mutation rate $0 < \mu < 1/2$, the faster the convergence to the solution $\tilde{p}_u = 1/2$.

4. Assortative mating

When mating between individuals differing at both loci is forbidden, the compatibility–viability selection rates $w_{h_1:h_2}$ are calculated by setting

$$w_{h_1:h_2} = \begin{cases} 0 & \text{for } h_1\text{: } h_2 = AB\text{: } ab \text{ or } h_1\text{: } h_2 = Ab\text{: } aB \\ w_{AM} & \text{otherwise.} \end{cases} \tag{20}$$

To obtain w_{AM} we impose again the constraint of a constant population size, which yields

$$w_{AM} = \frac{2}{N}\frac{1}{1-2\Delta^t}, \tag{21}$$

where

$$\Delta^t \equiv \frac{N^t_{AB}N^t_{ab} + N^t_{Ab}N^t_{aB}}{N^2} = p^t_{AB}p^t_{ab} + p^t_{Ab}p^t_{aB}. \tag{22}$$

Equations for the haplotypes frequencies are derived in the same way as in Ref. [15], and result in

$$p^{t+1}_{AB} = \frac{p^t_{AB}(1-\mu) + p^t_{ab}\mu + \Gamma^t\mu(1-\mu) - p^t_{AB}p^t_{ab}}{1-2\Delta^t} \tag{23}$$

$$p^{t+1}_{Ab} = \frac{p^t_{Ab}(1-\mu) + p^t_{aB}\mu - \Gamma^t\mu(1-\mu) - p^t_{Ab}p^t_{aB}}{1-2\Delta^t} \tag{24}$$

$$p^{t+1}_{aB} = \frac{p^t_{aB}(1-\mu) + p^t_{Ab}\mu - \Gamma^t\mu(1-\mu) - p^t_{aB}p^t_{Ab}}{1-2\Delta^t} \tag{25}$$

$$p^{t+1}_{ab} = \frac{p^t_{ab}(1-\mu) + p^t_{AB}\mu + \Gamma^t\mu(1-\mu) - p^t_{ab}p^t_{AB}}{1-2\Delta^t}. \tag{26}$$

Inserting the ansatz $p_{u'u''} = 1/4$ in these equations, it is straightforward to check that the equiprobable distribution is again an equilibrium solution. However, the stability analysis displays now a different outcome. Specifically, all eigenvalues are amplified by the factor 4/3 (coming from the denominator), giving rise to two degenerated eigenvalues $\zeta_{\mathrm{d}} = \frac{4}{3}(1-2\mu)$, and to a non degenerated eigenvalue $\zeta_{\mathrm{nd}} = \frac{2}{3}(1-2\mu)^2$. Accordingly, there is still a direction in which the movement is stable. However, in the 2-dimensional space spanned by the eigenvectors associated to ζ_{d} the stability depends on the mutation rate. For $\mu < 1/8$, $\zeta_d > 1$ and the fixed point turns out to be an unstable saddle. The change in a fixed point stability is the signature of a bifurcation. In this case the stable fixed point becomes unstable, which is associated with the appearance of new fixed points below $\mu_{\mathrm{crit}} = 1/8$, changing the global characteristics of the phase space. The analysis of these new equilibria and the implications of the dynamics is discussed in the following sections.

4.1. Fixed points for $\mu < 1/8$

To provide a comprehensive description of the fixed points of the map given by Eqs. (23)–(26) it is useful to divide them in 3 main families, which are enumerated below (derivation of the corresponding formulas is detailed in Appendix B). The color labels refer to Fig. 1, where the coordinate p_{ab} is eliminated through the normalization of the probabilities. This procedure gives the phase space the geometry of a tetrahedron of faces $p_{AB} = 0$, $p_{Ab} = 0$, $p_{aB} = 0$ and $p_{AB} + p_{Ab} + p_{aB} = 1$.

1. **First family—continuous sets of stable fixed points.**
   E_A (purple curves):

$$p_{AB} = \frac{1}{2}\left[1 - w_A - \lambda_A - \sqrt{(1-w_A-\lambda_A)^2 - 4(\mu - w_A\lambda_A)}\right]; \qquad p_{Ab} = w_A$$

$$p_{ab} = \frac{1}{2}\left[1 - w_A - \lambda_A + \sqrt{(1-w_A-\lambda_A)^2 - 4(\mu - w_A\lambda_A)}\right]; \qquad p_{aB} = \lambda_A$$

   E_B (blue curves):

$$p_{AB} = \frac{1}{2}\left[1 - w_B - \lambda_B - \sqrt{(1-w_B-\lambda_B)^2 - 4(\mu - w_B\lambda_B)}\right]; \qquad p_{aB} = w_B$$

$$p_{ab} = \frac{1}{2}\left[1 - w_B - \lambda_B + \sqrt{(1-w_B-\lambda_B)^2 - 4(\mu - w_B\lambda_B)}\right]; \qquad p_{Ab} = \lambda_B$$

   E_a (red curves):

$$p_{aB} = \frac{1}{2}\left[1 - w_a - \lambda_a - \sqrt{(1-w_a-\lambda_a)^2 - 4(\mu - w_a\lambda_a)}\right]; \qquad p_{ab} = w_a$$

$$p_{Ab} = \frac{1}{2}\left[1 - w_a - \lambda_a + \sqrt{(1-w_a-\lambda_a)^2 - 4(\mu - w_a\lambda_a)}\right]; \qquad p_{AB} = \lambda_a$$

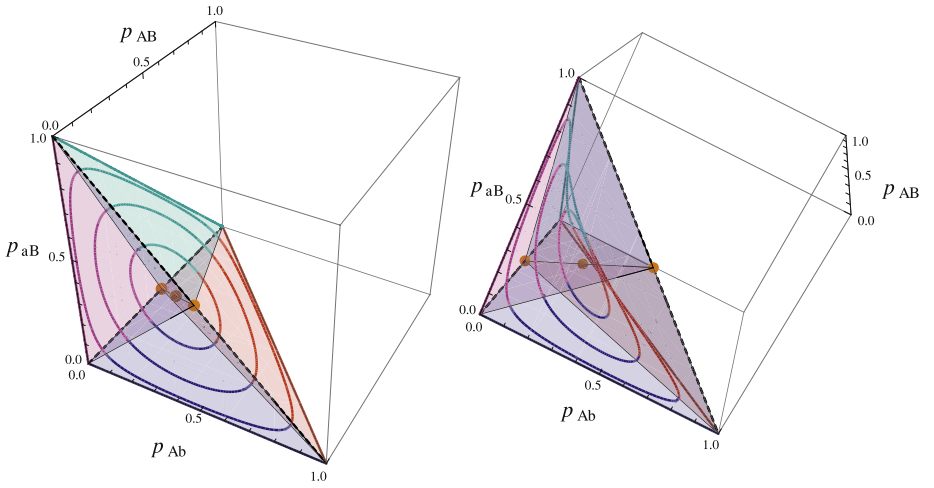

Fig. 1. (Color on-line) Two visualizations of the phase space, the stable equilibrium curves, and the unstable fixed points. The curves comprise the fixed points E_a (purple), E_b (blue), E_A (red) and E_B (cyan), and correspond to different mutation rates ($\mu = 0, 0.01, 0.05, 0.1$ from outside to inside). Unstable fixed points EU_1 and EU_2 corresponding to $\mu = 0$ are represented by orange circles, and the saddle point ES by a brown circle. The left panel displays four colored regions representing the basins of attraction of the corresponding equilibrium curves. In the right panel, the angle of observation is modified to highlight the 3D nature of the stable equilibrium curves.

E_b (cyan curves):

$$p_{Ab} = \frac{1}{2}\left[1 - w_b - \lambda_b - \sqrt{(1 - w_b - \lambda_b)^2 - 4(\mu - w_b\lambda_b)}\right]; \qquad p_{ab} = w_b$$

$$p_{aB} = \frac{1}{2}\left[1 - w_b - \lambda_b + \sqrt{(1 - w_b - \lambda_b)^2 - 4(\mu - w_b\lambda_b)}\right]; \qquad p_{AB} = \lambda_b$$

with

$$w_u = \frac{\mu(1 - \mu - \lambda_u)}{\mu + \lambda_u(1 - 2\mu)}, \tag{27}$$

for $u = a, b, A, B$. In all cases the range of λ_u is

$$x \le \lambda_u \le 1/2 - x + \sqrt{(1/2 - x)^2 + (x^2 - \mu)} \tag{28}$$

with

$$x = \frac{\mu}{1 - 2\mu}\left(\sqrt{\frac{1 - 2\mu + 2\mu^2}{\mu}} - 1\right). \tag{29}$$

For a given μ, these four continuous sets represent portions of a closed curve delimited by the following points:

$$E_{AB} = E_A \cap E_B\colon p_{AB} = 1/2 - x - \sqrt{(1/2 - x)^2 + (x^2 - \mu)}, \qquad p_{Ab} = p_{aB} = x,$$
$$p_{ab} = 1/2 - x + \sqrt{(1/2 - x)^2 + (x^2 - \mu)}$$
$$E_{aB} = E_a \cap E_B\colon p_{aB} = 1/2 - x - \sqrt{(1/2 - x)^2 + (x^2 - \mu)}, \qquad p_{AB} = p_{ab} = x,$$
$$p_{Ab} = 1/2 - x + \sqrt{(1/2 - x)^2 + (x^2 - \mu)}$$
$$E_{ab} = E_a \cap E_b\colon p_{ab} = 1/2 - x - \sqrt{(1/2 - x)^2 + (x^2 - \mu)}, \qquad p_{Ab} = p_{aB} = x,$$
$$p_{AB} = 1/2 - x + \sqrt{(1/2 - x)^2 + (x^2 - \mu)}$$
$$E_{Ab} = E_A \cap E_b\colon p_{Ab} = 1/2 - x - \sqrt{(1/2 - x)^2 + (x^2 - \mu)}, \qquad p_{AB} = p_{ab} = x,$$
$$p_{aB} = 1/2 - x + \sqrt{(1/2 - x)^2 + (x^2 - \mu)}.$$

By eliminating the variable p_{ab} through the normalization of the probabilities, the phase space adopts the geometry of a tetrahedron of faces $p_{AB} = 0$, $p_{Ab} = 0$, $p_{aB} = 0$ and $p_{AB} + p_{Ab} + p_{aB} = 1$ (see Fig. 1), whose vertices correspond to the four points obtained in this limit (points E_{ab}, E_{Ab}, E_{AB} and E_{aB} of Ref. [15]).

2. **Second family—unstable points (orange points)**

$$EU_1\colon p_{AB} = p_{ab} = z, \qquad p_{Ab} = p_{aB} = 1/2 - z$$

$$EU_2\colon p_{AB} = p_{ab} = 1/2 - z, \qquad p_{Ab} = p_{aB} = z$$

with

$$z = \frac{1}{4}\left(1 + \sqrt{1 + 8\mu(1-\mu)}\right).$$

Since $z \geq 1/2$ for any $\mu \geq 0$, it follows that $1/2 - z \leq 0$ and the only possible solutions of this type are those with μ strictly equal to zero, corresponding to the fixed points EU_1 and EU_2 of Ref. [15]. However, for mathematical purposes, we will still refer to these points as EU_1 and EU_2 for $\mu > 0$ even when they have no biological significance.

3. **Third family—saddle point, the equiprobable equilibrium (brown point)**

$$ES\colon p_{AB} = p_{Ab} = p_{aB} = p_{ab} = 1/4.$$

As $\mu \to 1/8$, x goes to $1/4$ and the stable equilibrium curves (together with the points E_{AB}, E_{Ab}, E_{aB} and E_{ab}) converge to the point ES which, as mentioned in the previous section, becomes stable.

4.2. Dynamics

To understand how the haplotype frequencies evolve in time and reach a specific equilibrium point we look at the allele frequencies. By means of Eqs. (23)–(26) it follows that

$$\begin{aligned}\tilde{p}_A^{t+1} &= p_{AB}^{t+1} + p_{Ab}^{t+1} \\ &= \frac{(1-\mu)(p_{AB}^t + p_{Ab}^t) + \mu(p_{ab}^t + p_{aB}^t) - (p_{AB}^t p_{ab}^t + p_{Ab}^t p_{aB}^t)}{1 - 2\Delta^t} \\ &= \frac{(1-\mu)\tilde{p}_A^t + \mu(1-\tilde{p}_A^t) - \Delta^t}{1 - 2\Delta^t}.\end{aligned} \tag{30}$$

Subtracting $1/2$ we obtain

$$\tilde{p}_A^{t+1} - \frac{1}{2} = \frac{(1-2\mu)\left(\tilde{p}_A^t - 1/2\right)}{1 - 2\Delta^t}. \tag{31}$$

The equations for the remaining allele frequencies are obtained in the same way and have exactly the same form.

Dividing the equation corresponding to $\tilde{p}_A$ by the equation corresponding to $\tilde{p}_B$ we find that the quantity

$$T \equiv \frac{\tilde{p}_A - 1/2}{\tilde{p}_B - 1/2} \tag{32}$$

represents a constant of motion. The existence of this constraint indicates that the trajectories of the haplotype frequencies are restricted to a plane of motion, a result known to hold for $\mu = 0$ [15]. Any of these planes contains the straight line connecting EU_1 and EU_2 and passing through ES. This line can be parametrized as

$$p_{AB} = 1/4 + \tau; \qquad p_{Ab} = p_{aB} = 1/4 - \tau \tag{33}$$

and passes through ES for $\tau = 0$ and through EU_1 and EU_2 for $\tau = \pm(z - 1/4)$, respectively. To verify that this line is contained in the plane of motion even for $\mu \neq 0$ it suffices to check that it satisfies the linear relation

$$(p_{AB} + p_{aB} - 1/2)T = p_{AB} + p_{Ab} - 1/2. \tag{34}$$

Given an initial condition, it is possible to calculate the constant T and to determine the corresponding plane of motion. Any of these planes intersects only two equilibrium points, either belonging to the sets E_b and E_B if $|T| < 1$, to the sets E_a and E_A if $|T| > 1$, corresponding to E_{AB} and E_{ab} if $T = 1$ or to E_{Ab} and E_{aB} if $T = -1$. Therefore, once the pair E_b—E_B, E_a—E_A, E_{AB}—E_{ab} or E_{Ab}—E_{aB} has been selected by the value of T, it suffices to know which of the two points is going to be reached. In Ref. [15] it is proven that the basins of attraction of the stable equilibrium curves for $\mu = 0$ have the following properties

- $\tilde{p}_A$ is the allele at the smallest proportion in the purple region.
- $\tilde{p}_B$ is the allele at the smallest proportion in the light blue region.
- $\tilde{p}_a$ is the allele at the smallest proportion in the red region.
- $\tilde{p}_b$ is the allele at the smallest proportion in the purple region.

As these basins of attraction remain to be the same for $\mu \neq 0$ (because the different stable equilibrium curves are still contained in the corresponding basin of attraction), after calculating the value of the constant T, the fate of the initial condition will be unambiguously determined by establishing which of the four alleles is in the smallest proportion. For instance, if $|T| < 1$ and the allele b is the one in the smallest proportion, by means of Eq. (32) we can write

$$T = \frac{-w_b + \lambda_b - \sqrt{(1 - w_b - \lambda_b)^2 - 4(\mu - w_b\lambda_b)}}{w_b - \lambda_b - \sqrt{(1 - w_b - \lambda_b)^2 - 4(\mu - w_b\lambda_b)}} \tag{35}$$

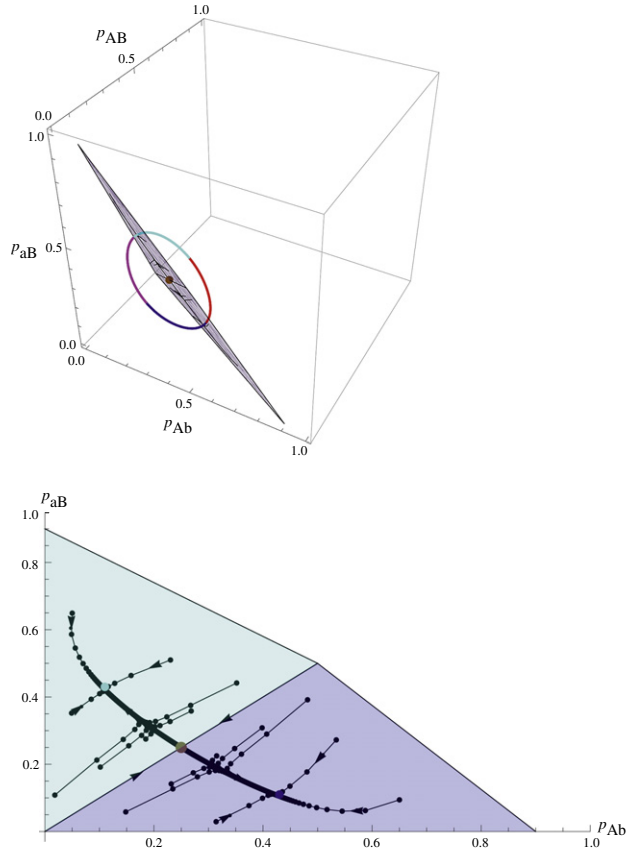

Fig. 2. (Color on-line) Top: Plane of motion for $T = -0.8$ and its intersection with the blue and cyan equilibrium curves, shown for $\mu = 0.1$. Bottom: projection of the trajectories on the plane $p_{AB} = 0$. The stable manifold of ES is shown with black arrows, together with several numerically integrated trajectories (black dots connected by lines).

which can be solved for λ_b to establish the equilibrium point. A similar equation for λ_B is obtained if the allele B is the one at the smallest proportion. If $|T| > 1$, depending on which among the alleles A and a is in the smallest proportion we determine the equations for the parameters λ_A and λ_a, respectively. Finally, if $T = 1$ we need to compare any of the pairs $A{-}a$ and $B{-}b$ to distinguish between the equilibria E_{AB} and E_{ab} (the point E_{AB} has both alleles A and B in smaller proportions than a and b), and if $T = -1$ we need to compare any of the pairs $A{-}b$ and $B{-}a$ (the point E_{Ab} has both alleles A and b in smaller proportions than a and B, and the point E_{aB} has both alleles a and B in smaller proportions than A and b). For example, for $T = 1$ and A and B in smaller proportions than a and b the attained fixed point will be E_{AB} (with x defined in Eq. (29)).

Fig. 2 shows the plane of motion for $T = -0.8$ and the equilibrium curves for $\mu = 0.1$ (top) and the projection of this plane into the plane $p_{AB} = 0$. The black dots connected by lines show numerically calculated trajectories that quickly approach a line perpendicular to the stable manifold of ES and then slowly move toward one of the stable equilibria, represented by the blue and cyan dots.

For $\mu < \mu_{\text{crit}} = 1/8$, the phase space has the same features than in Ref. [15], a foliation into planes of motion, where the trajectories are contained, and a separation into four regions, which are the basins of attraction of the four sets of points of type 1 (colored regions in Fig. 1). For $\mu = 0$ the colored attractors correspond to four edges of the phase space and represent solutions for which the population loses one allele, being the initially at the smallest proportion allele the one that vanishes. As the mutation rate increases, the attractors are deformed into curves located inside the phase space. The allele that initially was at the smallest proportion reaches an equilibrium value in which it is still the less abundant allele. As the attractors have no points representing the extinction of an allele, evolution makes initially extinct alleles to reappear to reach a non-zero equilibrium proportion as a consequence of mutations. A relevant question is how small is the equilibrium proportion of the initially less abundant allele for a given mutation rate μ. In fact, there is not one, but a range of possible equilibrium values depending on plane of motion where the initial condition is located (the specific value of T). There is a minimum value corresponding to the midpoint of set E_b ($T = 0$) and a maximum value corresponding to the extremes ($|T| = 1$, points E_{ab} and E_{Ab}). This is illustrated in Fig. 3 for the blue region, where allele b is at the highest proportion and allele B is at the smallest proportion.

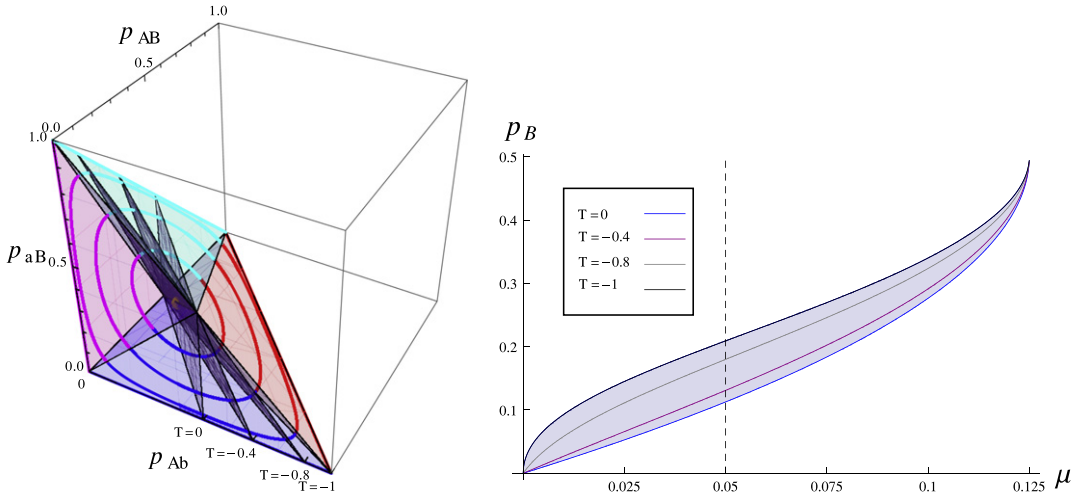

Fig. 3. (Color on-line) Proportion of the allele B at equilibrium in the blue region of the phase space. Notice that, except for $\mu = 0$ (for which $\tilde{p}_B = 0$ at equilibrium) and for $\mu = 1/8$ (for which $\tilde{p}_B = 1/2$ at equilibrium), all intermediate μ values have a minimum and a maximum $\tilde{p}_B$ value at equilibrium, corresponding to the planes having $T = 0$ and to the $|T| = 1$, respectively.

5. Bifurcation analysis

The global behavior of the dynamical system described by Eqs. (23)–(26) can be summarized with a very simple geometrical construction based on a bifurcation analysis. Consider first a plane motion, as that shown in Fig. 2, and a smooth coordinate transformation bringing the part of the plane inside the tetrahedron into a disk.

We will consider situations where $\mu > 0$ and also where $\mu < 0$. The continuation of the solutions for $\mu < 0$ is exclusively for mathematical purposes and does not represent a biological situation. In the latter scenario the stable equilibrium curves cross the plane outside the disk-shaped phase space, or outside the tetrahedron, which by construction represents probabilities that are negative or greater than one for at least one of the variables (blue point E_b and cyan point E_B in Fig. 4, left panel). For $\mu > 0$ we have again equilibrium points placed outside the phase space (Fig. 4, right panel), this time the orange unstable points EU_1 and EU_2. However, the identification of these points is still useful. This is because the direction pointing from any stable fixed point to EU_1 and EU_2 coincides with the orientation of the eigenvectors of the stability matrix of the corresponding stable point. This was proven for $\mu = 0$ [15] and remains true for $\mu > 0$ if the unstable points are prolonged outside the phase space.

In Fig. 5 we summarize all previous statements in a bifurcation analysis. As $\mu \to \mu_{\text{crit}} = 1/8$ from the left (Fig. 5, right panel) the stable points approach the central (brown) point ES along the unstable manifold of the latter. For $\mu > \mu_{\text{crit}}$ stable points disappear (the coordinates of the points become complex) and ES becomes stable. This represents a supercritical pitchfork bifurcation at $\mu_{\text{crit}} = 1/8$ along the central-stable direction (horizontal in the graph, connecting the stable points to ES). Now, if we look in the unstable-central direction (vertical in the graph, connecting ES with the unstable points), as $\mu \to \tilde{\mu}_{\text{crit}} \approx -0.112$ a similar behavior occurs (Fig. 5, left panel), except that along this direction the central point ES is stable and becomes unstable when $\mu < \tilde{\mu}_{\text{crit}}$, as the unstable points merge with ES and disappear. Accordingly, along the central-unstable direction the system displays a subcritical pitchfork bifurcation at $\tilde{\mu}_{\text{crit}}$. Middle panel of Fig. 5 displays a three-dimensional diagram showing the whole bifurcation structure of the dynamical system.

6. Discussion

This paper discusses the dynamical behavior of the haplotype frequencies for infinitely large populations subjected to mutations and assortative mating. Individuals are haploid with two biallelic loci and assortativity is included by preventing mating between individuals differing at both loci.

As shown in Section 4, stable equilibrium solutions do not correspond to isolated sets of haplotype frequencies, but to continuum curves. These curves are displayed in Fig. 1, and are similar to the case $\mu = 0$, where one of the alleles evolves into fixation. For $\mu \neq 0$ the locus at which one allele would be fixed remains polymorphic, and this makes the $\mu = 0$ curves to deform toward the interior of the phase space. The basins of attraction of the equilibrium curves, however, are independent of μ.

Interestingly, for all models studied here and in Ref. [15] the function T defined in Eq. (32) is a constant of motion. For panmictic populations and $\mu = 0$ this result is straightforward, since each allele frequency is conserved by the Hardy–Weinberg equilibrium law [31,32] adapted to two loci haploid populations. For panmictic populations and $\mu > 0$ this is still true, as can be seen from Eq. (19). Finally, Section 4.2 demonstrates that within the framework of an assortative

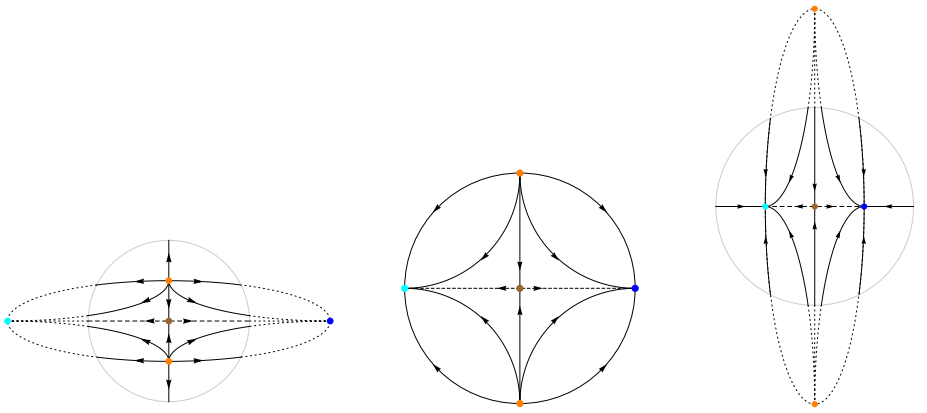

Fig. 4. (Color on-line) Schematic representation of the dynamics on a plane of motion. Left: $\tilde{\mu}_{\text{crit}} < \mu < 0$; Center: $\mu = 0$; Right: $0 < \mu < \mu_{\text{crit}}$. Except for the case $\mu = 0$ in which the phase space boundary is covered by trajectories, in the other cases the phase space boundary is represented by a gray circle. All trajectories are displayed in solid-black, with an arrow indicating the direction of movement. Dashed lines represent the unstable manifold of the fixed point *ES* (brown). Dotted lines are the prolongations of the trajectories (as well as prolongations of the manifolds of *ES*) outside the phase space. Blue and cyan points are stable fixed points, whereas orange points are unstable (*EU* points). The ellipses become lines at $\tilde{\mu}_{\text{crit}} = 1/2 - \sqrt{3/8} \approx -0.112$ (left) and $\mu_{\text{crit}} = 1/8 = 0.125$ (right).

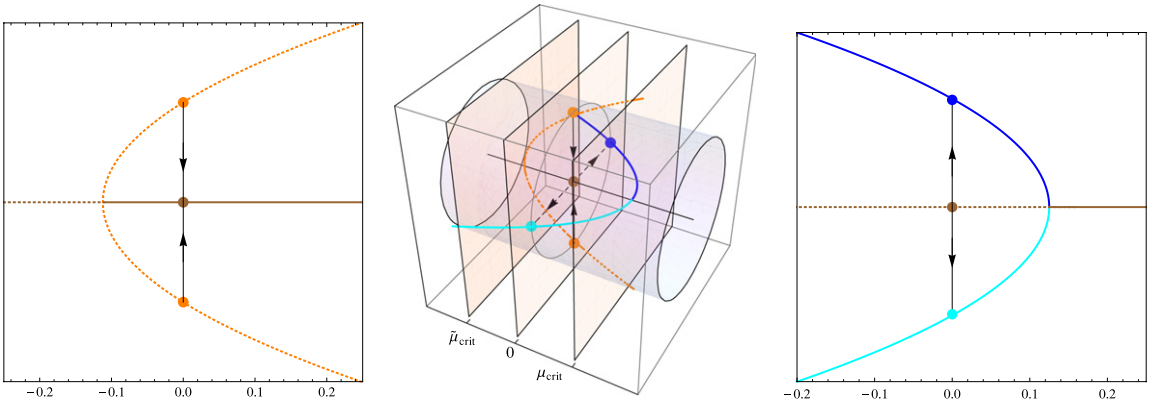

Fig. 5. (Color on-line) Bifurcation diagram, showing the two perpendicular pitchfork bifurcations (a supercritical, in the horizontal central-stable direction, superimposed to a subcritical in the vertical central-unstable direction). Notice that the central fixed point of both bifurcations coincides (point *ES*, in brown) and therefore the parameter axis of both bifurcations is the same. The horizontal cylinder represent the phase space constrained to a plane of motion, extended for the different values of the mutation rate μ. Stable and unstable manifolds of *ES* are explicitly depicted for the particular case $\mu = 0$.

Table 2
Effects of mutation and assortativity in allele frequencies.

	$\mu = 0$	$0 < \mu < \mu_{\text{crit}}$	$\mu_{\text{crit}} < \mu$
Random mating	HW-like	Equiprobable	
Assortative	Allele-correlation		Equiprobable

mating model T is constant as well, and that these results hold regardless of the presence of mutations, evidencing the robustness of the epistatic correlation introduced by assortativity.

As mentioned above, for $\mu < \mu_{\text{crit}} = 1/8$ the equilibrium solutions form continuous families and the conservation of T allows to determine which specific equilibrium is reached by an initial condition. These stable equilibrium curves merge at μ_{crit} and for $\mu > \mu_{\text{crit}}$ only the equiprobable solution exists.

It is interesting to observe that there is a trade off between mutations and assortativeness. Specifically, as μ increases and surpasses μ_{crit}, the effect of assortativeness disappears, and the population behaves as if mating were random. Table 2 compares the behavior of the population in different scenarios. We recognize three different regimes which we refer as the Hardy–Weinberg-like (HW-like) regime, in which allele frequencies do not change in time, the equiprobable regime, in which all allele frequencies are the same at equilibrium, and the allele-correlation regime, in which the evolution of an allele at one Lucas is affected by the evolution of the allele at the other locus through the conservation of T.

The bifurcation at $\mu_{crit} = 1/8$ has a very interesting biological interpretation within the context of the Eigen quasispecies model [33]. Specifically, by defining

$$w_{\alpha\alpha'} = 1 - p_{\beta\beta'} \tag{36}$$

where α and α' correspond to the alleles at the first and second locus, respectively, and β' and β' correspond to the their complementary (for instance, $\alpha = A$ implies $\beta = a$, and so on), the 4×4 matrix

$$Q_{\alpha_1,\alpha_1',\alpha_2,\alpha_2'} = \begin{cases} (1-\mu)^2 & \alpha_1 = \alpha_2 \text{ and } \alpha_1' = \alpha_2' \\ (1-\mu)\mu & \alpha_1 = \alpha_2 \text{ and } \alpha_1' \neq \alpha_2' \text{ or vice versa} \\ \mu^2 & \alpha_1 \neq \alpha_2 \text{ and } \alpha_1' \neq \alpha_2' \end{cases} \tag{37}$$

and the average fitness

$$\phi = \sum_{\alpha_1,\alpha_1'} w_{\alpha_1,\alpha_1'} p\alpha_1, \alpha_1', \tag{38}$$

it can be proved that the map

$$p_{\alpha_1\alpha_1'}^{t+1} = \sum_{\alpha_2\alpha_2'} p_{\alpha_2\alpha_2'} w_{\alpha_2\alpha_2'} Q_{\alpha_2\alpha_2',\alpha_1\alpha_1'} + (1-\phi) p_{\alpha_1\alpha_1'}, \tag{39}$$

up to the second order is identical to the map defined by Eqs. (23)–(26). This fact implies that both maps share the same fixed points and stability properties. Accordingly, the critical mutation rate obtained in Section 4 can be interpreted as an error threshold above which none of the haplotypes can fit in the population, leading to the so called error catastrophe. Two main differences must be stressed with respect to the standard quasispecies model. In the first place, in its original formulation the Eigen model considers individuals reproducing asexually, whereas in the present paper the reproduction is sexual. And in the second place, while in the original formulation the fitness landscape is constant in the course of evolution, in our model it has a dynamical structure, namely, it depends on the haplotype frequencies themselves (Eq. (36)). This is the reason why, depending on the initial conditions, below the critical mutation rate any of the haplotypes may end up being the most abundant, in contrast to the standard quasispecies model in which there is a master genotype with a fixed fitness that can adapt depending on the mutation rate. With those clarifications made, the connection between both scenarios is rigorous. Moreover, it is legitimate to compare the well known prediction of the quasispecies theory for the error threshold

$$\mu_{\text{crit}} \approx \frac{1}{L} \tag{40}$$

where L represents the genome size, with the result

$$\mu_{\text{crit}} = \frac{1}{8} = \frac{1}{4L} \tag{41}$$

obtained in this article. In a future publication we analyze a generalization of this model of assortative mating and mutations and examine how this result behaves for large genomes.

The analysis described in this paper holds for infinitely large populations only, where drift can be completely ignored. However, results for finite populations can be inferred by means of numerical simulations. The relevant parameter turns out to be μN, and four regimes must be analyzed: (i) for finite populations and $\mu = 0$ drift dominates and the only stable equilibria are those where both alleles are fixed, corresponding to four corners of the tetrahedron in Fig. 1; (ii) for $\mu N \ll 1$ both alleles evolve to near fixation, similar to the case $\mu = 0$; (iii) for $\mu N \approx 1$ drift and mutation balance each other and the haplotype distribution never equilibrates: the distribution moves in the neighborhood of the curve representing the continuum of equilibria for infinitely large populations (colored curves in Fig. 1). Finally, for (iv) $\mu N \gg 1$ the motion along the line of equilibria becomes extremely slow and the results for infinitely large populations are recovered. These results were confirmed by numerical simulations but seem to be particular of the case of 2 loci. A detailed discussion of these effects for arbitrary number of loci will be presented in a future publication.

Acknowledgments

This work was partly supported by FAPESP (Fundação de Amparo à Pesquisa do Estado de São Paulo) (2009/11032-5) and CNPq (Conselho Nacional de Desenvolvimento Científico e Tecnológico) (302858/2011-0).

Appendix A. Probabilities of offspring production

In this appendix we explain the coefficients in the third column of Table 1. Specifically, we discuss how mutations are incorporated to account for the total probability of offspring haplotypes. To do so, we will look at one locus at a time, and

without loss of generality we will consider the first locus, labeled by a single prime. For a given allele u' of the offspring there are three possibilities for the alleles u'_{h1} and u'_{h2} of the parents:

(a) $u'_{h1} = u'_{h2} \neq u'$. For the offspring to have an allele that is different from that inherited from its parents a mutation necessarily needs to take place. Therefore, the probability is lessened by a factor μ.
(b) $u'_{h1} = u'_{h2} = u'$. As the allele transmitted to the offspring coincides with the alleles of both parents, mutation cannot happen in this case. The contribution is thus through a factor $(1 - \mu)$.
(c) $u'_{h1} \neq u'_{h2}$. Since each parent has now a different allele, one of them is equal to u' and the other is different. So, the general contribution to the probability can be written as $(1/2)f_1(\mu) + (1/2)f_2(\mu)$, where $f_i(\mu)$ is either μ (if this allele mutates) or $1 - \mu$ (if it does not mutate). Since parent's alleles are different, $f_1 \neq f_2$ and $f_1 = 1 - f_2$. In conclusion, for any of the four different possibilities comprised in this case the contribution to the probability is through a factor $1/2$.

Therefore, for an offspring *AB* having both parents *AB* we have case (b) for both loci and the fraction of successful *AB* encounters is $w_{AB:AB} \times (1 - \mu)^2$. If the parents are *AB* and *Ab* instead, we have case (b) for the first locus and case (c) for the second, leading to $w_{AB:Ab} \times (1 - \mu) \times 1/2$.

The other cases in the table are obtained in a similar way, except when the parents have different alleles at both loci. In this case a recombination rate may be considered: with a probability r there is recombination of the alleles of the parents and with a probability $1 - r$ there is not. For example, if the parents are of types *Ab* and *aB* and the recombination does not occur, the transmitted haplotypes (before mutations) are *Ab* or *aB*, both with probability $1/2$. On the other hand, if the recombination takes place all possible haplotypes can occur with the same probability $(1/4)$.

Appendix B. Derivation of fixed points formulas

Consider Eqs. (23)–(26) subjected to the fixed point condition $p^{t+1}_{u'u''} = p^t_{u'u''} \equiv p_{u'u''}$.[1] Subtracting (23) from (26) and (24) from (25) we obtain, after some algebraic manipulations

$$(p_{AB} - p_{ab})(\Delta - \mu) = 0 \tag{B.1}$$
$$(p_{Ab} - p_{aB})(\Delta - \mu) = 0. \tag{B.2}$$

These equations are independent and thus need to be satisfied at the same time. Eq. (B.1) implies $p_{AB} = p_{ab}$ or $\mu = \Delta$, whereas Eq. (B.2) implies $p_{Ab} = p_{Ab}$ or $\mu = \Delta$. Accordingly, the following four different scenarios need to be considered separately:

(I) $p_{AB} = p_{ab}$, $p_{Ab} = p_{aB}$ and no constraints relating Δ and μ,
(II) $p_{AB} = p_{ab}$, $\mu = \Delta$ and no constraints relating p_{Ab} and p_{aB},
(III) $p_{Ab} = p_{aB}$, $\mu = \Delta$ and no constraints relating p_{AB} and p_{ab},
(IV) $\mu = \Delta$ and no constraints relating p_{AB} and p_{ab}, or p_{Ab} and p_{Ab}.

Adding Eqs. (23) and (26) on one hand, and (24) and (25) on the other hand, leads to

$$\Delta(p_{AB} + p_{ab}) = p_{AB}p_{ab} - \Gamma\mu(1 - \mu) \tag{B.3}$$
$$\Delta(p_{Ab} + p_{aB}) = p_{Ab}p_{aB} + \Gamma\mu(1 - \mu), \tag{B.4}$$

respectively. These equations, however, are equivalent. For instance, by subtracting Δ from both members of (B.3) and changing the sign, one gets Eq. (B.4). In what follows we will use one of these two equations according to the convenience and consider the four scenarios enumerated above.

(I) In this case $\Delta = p^2_{AB} + p^2_{Ab}$ and $\Gamma = 2p^2_{Ab} - 2p^2_{AB}$. Accordingly, Eq. (B.3) reads

$$2(p^2_{AB} + p^2_{ab})p_{AB} = p^2_{AB} - 2(p_{Ab} - p_{AB})\mu(1 - \mu). \tag{B.5}$$

Now, in the present situation normalization gives $p_{Ab} = 1/2 - p_{AB}$. Replacing this condition in (B.5) yields

$$0 = p^3_{AB} - \frac{3}{4}p^2_{AB} + p_{AB}\left[\frac{1}{8} - \frac{1}{2}\mu(1 - \mu)\right] + \frac{1}{8}\mu(1 - \mu), \tag{B.6}$$

whose solutions are

$$p_{AB} = p_{ab} = p_{Ab} = p_{aB} = \frac{1}{4} \tag{B.7}$$

[1] In what follows we will omit the superscript t.

or

$$p_{AB} = p_{ab} = \frac{1}{4}(1 \pm z) \tag{B.8}$$

$$p_{Ab} = p_{aB} = \frac{1}{2} - p_{AB} \tag{B.9}$$

with $z = \sqrt{1 + 8\mu(1-\mu)}$.

(II) These conditions lead to the points termed E_{aB} and E_{Ab}. We have $\Gamma = p_{Ab}^2 + p_{aB}^2 - 2p_{AB}^2$, which makes Eq. (B.3) take the form

$$2\mu p_{AB} = p_{AB}^2 - (p_{Ab}^2 + p_{aB}^2 - 2p_{AB}^2)\mu(1-\mu). \tag{B.10}$$

From the normalization condition $1 = 2p_{AB} + p_{Ab} + p_{aB}$ and the constraint $\mu = \Delta = p_{AB}^2 + p_{Ab}p_{aB}$ we can write

$$p_{Ab}^2 + p_{aB}^2 = (1 - 2p_{AB})^2 - 2(\mu - p_{AB}^2) \tag{B.11}$$

and substitute in (B.10) to obtain a closed formula for p_{AB}:

$$0 = p_{AB}^2 + \frac{2\mu}{1-2\mu}p_{AB} - \frac{\mu(1-2\mu)}{1-2\mu}. \tag{B.12}$$

The solution is

$$p_{AB} = p_{ab} \equiv x \tag{B.13}$$

with

$$x = \frac{\mu}{1-2\mu}\left[\sqrt{\frac{1-2\mu+2\mu^2}{\mu}} - 1\right]. \tag{B.14}$$

Now, by eliminating one the two remaining variables through the normalization and the relation $\Delta = \mu$, one arrives to

$$p^2 - (1-2x)p - (x^2 - \mu) = 0 \tag{B.15}$$

where p stands either for p_{Ab} or for p_{aB}. As the previous equation is satisfied by two different values of p, namely,

$$p = 1/2 - x \pm \sqrt{(1/2-x)^2 + (x^2-\mu)} \tag{B.16}$$

the solutions in this case are split into two. Choosing $p = p_{AB}$ and, for instance, the plus sign, the solution becomes

$$\begin{aligned} p_{AB} &= p_{ab} \equiv x, \\ p_{Ab} &= 1/2 - x + \sqrt{(1/2-x)^2 + (x^2-\mu)}, \\ p_{aB} &= 1/2 - x - \sqrt{(1/2-x)^2 + (x^2-\mu)}. \end{aligned} \tag{B.17}$$

The minus sign gives instead

$$\begin{aligned} p_{AB} &= p_{ab} \equiv x, \\ p_{Ab} &= 1/2 - x - \sqrt{(1/2-x)^2 + (x^2-\mu)}, \\ p_{aB} &= 1/2 - x + \sqrt{(1/2-x)^2 + (x^2-\mu)}. \end{aligned} \tag{B.18}$$

The same two solutions are obtained by choosing $p = p_{aB}$, however in the opposite order in relation to the sign chosen in (B.16).

(III) These conditions lead to the fixed points termed E_{AB} and E_{ab}. The demonstration is equivalent to the previous one.

(IV) This condition lead to the continuous set of fixed points of the first family. The constraint is just $\Delta = \mu$ (and the normalization $1 = p_{AB} + p_{Ab} + p_{aB} + p_{ab}$). Now, by eliminating for instance p_{aB} (from the definition of Δ), we can write

$$p_{AB}p_{ab} + p_{Ab}(1 - p_{AB} - p_{Ab} - p_{ab}) = \mu \tag{B.19}$$

or

$$p_{Ab}^2 - (1 - p_{AB} - p_{ab})p_{Ab} + (\mu - p_{AB}p_{ab}) = 0. \tag{B.20}$$

On the other hand, by combining the constraint $\Delta = \mu$ with Eq. (B.3), and again eliminating p_{aB} through the normalization condition leads to

$$p_{Ab}^2 - (1 - p_{AB} - p_{ab})p_{Ab} - \frac{1-2\mu}{2(1-\mu)}(p_{AB} + p_{ab}) - \frac{1-2\mu+2\mu^2}{2\mu(1-\mu)}p_{AB}p_{ab} + \frac{1}{2} = 0. \tag{B.21}$$

By comparing Eqs. (B.20) and (B.21), we get

$$\mu - p_{AB}p_{ab} = -\frac{1-2\mu}{2(1-\mu)}(p_{AB}+p_{ab}) - \frac{1-2\mu+2\mu^2}{2\mu(1-\mu)}p_{AB}p_{ab} + \frac{1}{2} \tag{B.22}$$

which means

$$p_{ab} = \frac{\mu(1-\mu-p_{AB})}{\mu + p_{AB}(1-2\mu)} \tag{B.23}$$

or

$$p_{AB} = \frac{\mu(1-\mu-p_{ab})}{\mu + p_{ab}(1-2\mu)}. \tag{B.24}$$

Now, as all the information available was employed, we must conclude that the fixed points we are concerning are not single points but represent 1-dimensional sets in the 3-dimensional phase space. Accordingly, we can take one of the variables to parametrize this 1-dimensional set. As Eqs. (B.23) and (B.24) are equivalent, we take the first one and describe the fixed points through the parametrization $p_{AB} = \lambda$ and $p_{ab} = w(\lambda) = \frac{\mu(1-\mu-\lambda)}{\mu+\lambda(1-2\mu)}$. To obtain the remaining variables, we simply solve (B.20) for p_{Ab}. This gives

$$p_{Ab} = v_{\pm}(\lambda) \equiv \frac{1}{2}\left[1 - w(\lambda) - \lambda \pm \sqrt{(1-w(\lambda)-\lambda)^2 - 4(\mu - w(\lambda)\lambda)}\right]. \tag{B.25}$$

Now, a little algebra allows to see that

$$1 - (\lambda + w(\lambda) + v_+(\lambda)) = v_- \tag{B.26}$$

which means that one possible solution is of the form

$$p_{AB} = \lambda; \qquad p_{ab} = w(\lambda) \qquad p_{Ab} = v_+ \quad \text{and} \quad p_{aB} = v_-. \tag{B.27}$$

This solution corresponds to the set E_A of Section 4.1. If we take $p_{Ab} = v_-$, the relation (B.26) means $p_{aB} = v_+$, and the solution corresponds to the set of fixed points E_B.
The other two remaining sets of fixed points, E_a and E_b, can be obtained by the same procedure by eliminating variables p_{AB} or p_{ab}.
The limits of each set of continuous solutions are given by the points in the phase space where $p_{AB} = p_{ab}$ and $p_{Ab} = p_{aB}$, i.e. the points where the continuous sets touch. For instance, for the set E_A the condition $p_{AB} = p_{ab}$ gives the lower limit of λ_A,

$$\begin{aligned} &\lambda_A^* = w(\lambda_A^*) \\ &\lambda_A^* = x = \frac{\mu}{1-2\mu}\left[\sqrt{\frac{1-2\mu+2\mu^2}{\mu}} - 1\right], \end{aligned} \tag{B.28}$$

and the condition $p_{Ab} = p_{aB}$ gives the upper limit of λ_A,

$$\begin{aligned} &(1-w-\lambda_A^*)^2 - 4(\mu - w\lambda_A^*) = 0 \\ &\lambda_A^* = \frac{1}{2} - x + \sqrt{\left(\frac{1}{2}-x\right)^2 - (\mu - x^2)}, \end{aligned} \tag{B.29}$$

which correspond to the points E_{AB} and E_{Ab}, respectively.

Appendix C. The stable manifold of *ES*

The line connecting EU_1 and EU_2 passing through ES can be parametrized by τ as

$$p_{AB} = p_{ab} = 1/4 + \tau; \qquad p_{Ab} = p_{aB} = 1/4 - \tau. \tag{C.1}$$

It passes through ES for $\tau = 0$ and through EU_1 and EU_2 for $\tau = z - 1/4$ and $\tau = -z + 1/4$, respectively. Consider an initial condition on this line. Substituting the above values of haplotype frequencies into the dynamical equations (23)–(26) it is possible to rewrite them as

$$p_{AB}^{t+1} = p_{ab}^{t+1} = 1/4 + \tau'; \qquad p_{Ab}^{t+1} = p_{aB}^{t+1} = 1/4 - \tau' \tag{C.2}$$

with

$$\tau' = \frac{2}{3}\tau\left(\frac{1-4\mu(1-\mu)}{1-16\tau^2/3}\right). \tag{C.3}$$

This shows that the line is an invariant curve, since points that started on the line remain on the line. The fixed points of the dynamics are obtained by setting $\tau' = \tau$ and result in $\tau = 0$ and $\tau = \pm(z - 1/4)$, i.e. the points ES, EU_1 and EU_2. Since the last two are totally unstable, generic points on the line in the interval $-(z - 1/4) < \tau < +(z - 1/4)$ converge to ES and are, therefore, its stable manifold.

References

[1] J.A. Coyne, H.A. Orr, Speciation, first ed., Sinauer Associates, Inc., 2004.
[2] P. Nosil, Ecological Speciation, Oxford University Press, Oxford, New York, 2012.
[3] E. Mayr, What Evolution Is, Basic Books, 2001.
[4] M.A.M. de Aguiar, M. Baranger, E.M. Baptestini, L. Kaufman, Y. Bar-Yam, Global patterns of speciation and diversity, Nature 460 (2009) 384–387.
[5] A.B. Martins, M.A.M.d. Aguiar, Y. Bar-Yam, Evolution and stability of ring species, Proc. Nat. Acad. Sci. 110 (2013) 5080–5084.
[6] E.M. Baptestini, M.A.M. de Aguiar, Y. Bar-Yam, The role of sex separation in neutral speciation, J. Theor. Ecol. 6 (2013) 213.
[7] A.S. Kondrashov, M. Shpak, On the origin of species by means of assortative mating, Proc. R. Soc. B 265 (1998) 2273.
[8] S. Gavrilets, H. Li, M.D. Vose, Rapid parapatric speciation on holey adaptive landscapes, Proc. Biol. Sci. 265 (1998) 1483–1489.
[9] S. Gavrilets, H. Li, M.D. Vose, Patterns of parapatric speciation, Proc. Biol. Sci. 54 (2000) 1126–1134.
[10] U. Candolin, The use of multiple cues in mate choice, Biol. Rev. 78 (2003) 575–595.
[11] S. Wright, Isolation by distance, Genetics 28 (1943) 114–138.
[12] M.A.M. de Aguiar, Y. Bar-Yam, The Moran model as a dynamical process on networks and its implications for neutral speciation, Phys. Rev. E 84 (2011) 031901.
[13] E.M. Baptestini, M.A.M. de Aguiar, Y. Bar-Yam, Conditions for neutral speciation via isolation by distance, J. Theoret. Biol. 335 (2013) 51.
[14] M.A.M. de Aguiar, D.M. Schneider, E. do Carmo, P.R.A. Campos, A.B. Martins, Error catastrophe in populations under similarity-essential recombination, 2014, submitted for publication.
[15] D.M. Schneider, A.B. Martins, E. do Carmo, M.A.M. de Aguiar, Toward a theory of topopatric speciation: the role of genetic assortative mating, Physica A 409 (2014) 35–47.
[16] M. Kimura, A model of a genetic system which leads to closer linkage by natural selection, Evolution 10 (1956) 278–287.
[17] J.F. Crow, M. Kimura, An Introduction to Population Genetics Theory, The Blackburn Press, 1970.
[18] S. Karlin, General two-locus selection models: some objectives, results and interpretations, Theor. Popul. Biol. 7 (1975) 364–398.
[19] A. Hastings, Marginal underdominance at a stable equilibrium, Proc. Natl. Acad. Sci. USA 78 (1981) 6558–6559.
[20] W.J. Ewens, Mathematical Population Genetics: I. Theoretical Introduction, Springer, 2004.
[21] M. Hamilton, Population Genetics, first ed., Wiley–Blackwell, 2009.
[22] S. Gavrilets, Fitness Landscapes and the Origin of Species, Princeton University Press, 2004.
[23] P. O'Donald, Assortative mating in a population in which two alleles are segregating, Heredity 15 (1960) 389–396.
[24] J.L. Crosby, The evolution of gametic discontinuity: computer models of the selection of barriers to interbreeding between subspecies, Heredity 25 (1970) 253–297.
[25] J. Felsenstein, Skepticism towards Santa Rosalia, or why are there so few kinds of animals? Evolution 35 (1981) 124–138.
[26] W.S. Moore, A single locus mass-action model of assortative mating with comments on the process of speciation, Heredity 46 (1979) 191–195.
[27] F. Spirito, The reduction of gene exchange due to a prezygotic isolating mechanisms with monogenic inheritance, Theor. Popul. Biol. 32 (1987) 216–239.
[28] F. Spirito, F. Sampogna, Conditions for the maintenance of prezygotic and zygotic isolation in a continent–island model, Theor. Popul. Biol. 48 (1995) 235–250.
[29] P.G. Higgs, B. Derrida, Stochastic models for species formation in evolving populations, J. Phys. A 24 (1991) L985–L991.
[30] P.G. Higgs, B. Derrida, Genetic distance and species formation in evolving populations, J. Mol. Evol. 35 (1992) 454–465.
[31] G.H. Hardy, Mendelian proportions in a mixed population, Science 28 (1908) 49–50.
[32] W. Weinberg, Über den nachweis der vererbung beim menschen, Jh Ver Vaterl Naturk Wurttemb 64 (1908) 368–382.
[33] M. Eigen, J. McCaskill, P. Schuster, The molecular quasi-species, Adv. Chem. Phys. 75 (1989) 149–263.